

## Nicotinic acetylcholine receptor activation reduces skeletal muscle inflammation of *mdx* mice

Paulo Emílio Corrêa Leite<sup>a,c</sup>, Jussara Lagrota-Candido<sup>b</sup>, Louise Moraes<sup>d</sup>, Livia D'Elia<sup>c</sup>, Douglas Florindo Pinheiro<sup>b</sup>, Rafael Ferreira da Silva<sup>a,b</sup>, Edna N. Yamasaki<sup>c,1</sup>, Thereza Quirico-Santos<sup>a,\*</sup>

<sup>a</sup> Laboratório de Patologia Celular, Instituto de Biologia, Universidade Federal Fluminense, Niterói, Rio de Janeiro, Brazil

<sup>b</sup> Laboratório de Imunopatologia, Instituto de Biologia, Universidade Federal Fluminense, Niterói, Rio de Janeiro, Brazil

<sup>c</sup> Laboratório de Neurobiologia da Retina, Instituto de Biofísica Carlos Chagas Filho, Universidade Federal do Rio de Janeiro, Rio de Janeiro, Brazil

<sup>d</sup> Laboratório de Neurobiologia Celular e Molecular, Instituto de Biofísica Carlos Chagas Filho, Universidade Federal do Rio de Janeiro, Rio de Janeiro, Brazil

### ARTICLE INFO

#### Article history:

Received 6 March 2008

Received in revised 2 June 2010

Accepted 3 June 2010

#### Keywords:

Muscular dystrophy

*Mdx*

Acetylcholine receptor

Cytokine

Macrophage

Skeletal muscle

### ABSTRACT

*Mdx* mice develop an inflammatory myopathy characterized at different ages by myonecrosis with scattered inflammatory infiltrates followed by muscular regeneration and later persistent fibrosis. This work aimed to verify the putative anti-inflammatory role of nicotinic acetylcholine receptor (nAChR) in the *mdx* muscular lesion. Mitigation of myonecrosis and decreased TNF $\alpha$  production were accompanied by increased numbers of F4/80 macrophages expressing nAChR $\alpha$ 7. In vivo treatment with nicotine attenuated muscular inflammation characterized by reduced metalloprotease MMP-9 activity, TNF $\alpha$  and NF $\kappa$ B content and increased muscular regeneration. Our data indicate that nAChR activation influences local inflammatory responses in the muscular lesion of *mdx* mice.

© 2010 Elsevier B.V. All rights reserved.

### 1. Introduction

Duchenne muscular dystrophy (DMD) is a devastating X-linked recessive inflammatory myopathy in which progressive muscle degeneration is caused by a defect in the gene coding for dystrophin, a large cytoskeletal protein present in skeletal muscles and certain neurons (Voisin and de la Porte, 2004). At the sarcolemma, the dystrophin glycoprotein complex (DGC) shares a receptor for the extracellular matrix components laminin and agrin providing an important framework for spindle fiber differentiation, clustering and consolidation of acetylcholine receptors (AChRs) at the neuromuscular junction (Carlson, 1998; Williams and Jacobson, 2010). Lack of dystrophin causes sarcolemmal instability predisposing to myonecrosis and activation of inflammatory signalling cascades. Although inflammation is the pathological hallmark of dystrophic muscular lesion, the mechanisms influencing muscle fiber pathology are still not understood (Evans et al., 2009). Dystrophinopathy in *mdx* mice is

characterized by progressive muscle wasting, high plasma concentration of creatine kinase due to substantial muscle necrosis, calcium-dependent endplate degeneration and atrophy (Torres and Duchon, 1987). Cycles of myonecrosis with scattered inflammatory infiltrates and muscular regeneration are evident between 3 and 4 weeks followed by persistent fibrosis and accumulation of connective tissues from 12 weeks onwards in older *mdx* mice (Lagrota-Candido et al., 2002; Lefaucher and Sebillé, 1996; McGeachie and Grounds, 1999).

Inflammatory cells present a complete cholinergic system consisting of acetylcholine (ACh), muscarinic and nicotinic receptors, choline acetyl-transferase and acetyl-cholinesterase (Kawashima and Fujii, 2003; Tayebati et al., 2002). Nicotine acetylcholine receptors (nAChRs) belong to the family of nicotinic acetylcholine ligand-gated ion channels and have five subunits forming hetero- or homopentameric receptors with different pharmacological properties (Gotti and Clementi, 2004). Cholinergic stimulation of the  $\alpha$ 7 homopentameric nAChR inhibits production of pro-inflammatory cytokines (Bernik et al., 2002; Borovikova et al., 2000; Nizri et al., 2006; Saeed et al., 2005; Wang et al., 2003), expression of endothelial cell adhesion molecules, and leukocyte recruitment during inflammation (Saeed et al., 2005). The anti-inflammatory effect of nAChR $\alpha$ 7 stimulation is partly related to the regulation of cytokine production by macrophages (Bernik et al., 2002; Borovikova et al., 2000; Rosas-Ballina et al., 2009; Saeed et al., 2005; Shytle et al., 2004; Ulloa, 2005; Wang et al., 2003) and T lymphocytes (Nizri et al., 2006).

\* Corresponding author. Laboratory of Cellular Pathology, Institute of Biology, Federal Fluminense University, Niterói, RJ, 24020-141, Brazil. Tel.: +55 21 2629 2305; fax: +55 21 2629 2268.

E-mail addresses: [yamasaki.e@unic.ac.cy](mailto:yamasaki.e@unic.ac.cy) (E.N. Yamasaki), [tquirico@vm.uff.br](mailto:tquirico@vm.uff.br) (T. Quirico-Santos).

<sup>1</sup> Present address: Department of Life and Health Sciences, University of Nicosia, 46 Makedonitissas Ave, Nicosia, 1700 Cyprus.

Presence of acetylcholine as the neurotransmitter of cholinergic system at sites of nerve–muscle contacts establishes a link between immune and nervous system which might be influencing the pathogenesis of *mdx* muscular lesion. In the present study, we correlated nAChR $\alpha$ 7 expression with presence of F4/80 macrophages and local production of the inflammatory cytokine tumor necrosis factor alpha (TNF $\alpha$ ) at different stages of the disease and further determined the effect of in vivo stimulation of nicotinic acetylcholine receptors upon inflammation and muscular regeneration of *mdx* mice.

## 2. Materials and methods

### 2.1. Animal care

Male *mdx* dystrophic and age-matched C57BL/10J control non-dystrophic mice were maintained at the animal house facilities of the Department of Cellular and Molecular Biology at Fluminense Federal University. Mice were kept at constant temperature (20 °C) with a light/dark cycle of 12 h. Each cage housed up to 4 mice of the same age, gender and offspring to minimize stress. Mice were sacrificed at ages 2, 4, 12 and 24 weeks. All procedures were approved by the Institutional Animal Care (protocol 174-09) and were conducted according to Brazilian Ethics Guidelines for Animal Studies (COBEA).

### 2.2. Histological staining and morphometric analysis

Gastrocnemius muscles from *mdx* and control mice were carefully removed, fixed in formalin-buffered Millonig fixative (pH 7.2) for 24 h. Wax-embedded 5  $\mu$ m-thick sections were stained with hematoxylin–eosin and sirius red for collagen. Images of all cross-sections from five *mdx* and control mice at each time point were acquired with a microdigital camera mounted on a Zeiss Axioplan microscope (Zeiss, Oberkochen, Germany) using a 20 $\times$  objective. Images were mounted with Photomerge Adobe Photoshop CS3 software. Total surface area and areas occupied by inflammatory infiltrates, regeneration and collagen deposition were determined with Image-Pro 4.5 software. Regenerating fibers were identified by strong basophilic sarcoplasm and centrally located nuclei. Results were expressed as percentage of total area in the cross-section.

### 2.3. Immunohistochemistry

Mice were deeply anesthetized by intraperitoneal injection of (1:1) ketamine hydrochloride (Ketalar; Parke-Davis, São Paulo, Brazil) and xylazine hydrochloride (Rompun; Bayer, São Paulo, Brazil), perfused with 20 mL 0.25% heparin (Actparin; Bergamo, São Paulo, Brazil) in saline through the ascending aorta followed by 30 mL cold buffer fixative (4% paraformaldehyde in 100 mM PBS, pH 7.4). Muscles were carefully removed, placed for 4 h in 4% paraformaldehyde solution and submitted to cryoprotection by sequential incubation with a gradient of sucrose solution (10%, 20% and 30% w/v in PBS) for 6 h at 4 °C in each solution. Cryostat cross-sections (10  $\mu$ m, spaced 200  $\mu$ m) were mounted on poly-L-lysine pre-coated slides, rinsed for 20 min in PBS and incubated for 2 h with blocking buffer PBST (0.05% Triton X-100 in PBS, containing 5% normal goat or horse). For nAChR $\alpha$ 7 detection, sections were incubated overnight at 4 °C with primary monoclonal rat anti-nAChR $\alpha$ 7 (clone 319; Covance, Princeton, NJ) at 1:250 dilution in PBS followed by incubation with goat anti-rat IgG FITC (1:300 dilution; Invitrogen, Carlsbad, CA) for 2 h at 37 °C. Sections were further incubated during 2 h with rat anti-F4/80 biotinylated primary antibody at 1:40 dilution (clone A3-1 C57BL; Serotec, Oxford, UK) for detection of macrophages (Khazen et al., 2005), followed by 1 h incubation with streptavidin Cy3-conjugate (1:1000 dilution; Jackson Immuno Research; West Grove, PA) at room temperature. Muscular regeneration was evidenced by overnight incubation at 4 °C with goat anti-NCAM antibody (1:200 dilution; Santa Cruz Biotechnology, Santa Cruz, CA)

followed by incubation for 1 h at 37 °C with donkey anti-goat IgG Alexa 488-labeled antibody (1:200 dilution; Molecular probes, Eugene, OR). TOPRO-3 (Molecular probes, Eugene, OR) was always used to counterstain cellular nuclei. Images randomly collected from seven inflammatory foci or regeneration areas at each time point were obtained with Zeiss LSM510 META confocal microscope with identical time exposure and image settings. Analysis was performed using image-analysis software AxioVert 40 (Zeiss, Oberkochen, Germany). Five animals were included at each time point.

### 2.4. Western blotting

Skeletal muscles were homogenized with protease inhibitor buffer (Sigma, St Louis, MI). Protein extracts were clarified by centrifugation at 12,000  $\times$  g for 15 min at 4 °C, and quantification was determined by the Lowry method (Lowry et al., 1951) followed by concentration adjustment with sample buffer, pH 6.8 (173 mM Tris, 30% glycerol, 3% sodium dodecyl sulfate, 3%  $\beta$ -mercaptoethanol, and 0.1% bromophenol blue). Samples were denatured by boiling for 5 min and loaded on 10% SDS-PAGE for nAChR $\alpha$ 7 and myogenin, on 12.5% for TNF $\alpha$  and 7.5% for NCAM detection. Proteins were transferred to PVDF membranes (Hybond-P; Amersham Biosciences, Fairfield, CT) and blocked for 2 h at room temperature with 5% nonfat dry milk in 0.05% Tween 20 Tris-buffered saline (TBST), pH 7.4 on a rocking platform. Membranes were incubated with specific rat monoclonal anti-nAChR $\alpha$ 7 (clone 319 at 1:400 dilution; Covance, Princeton, NJ); anti-TNF biotinylated antibodies (clone MP6-XT3 at 1:3000 dilution; BD-Pharmingen Biosciences, San Diego, CA); polyclonal rabbit anti-NF $\kappa$ B p65 (at 1:500 dilution; Santa Cruz Biotechnology, Santa Cruz, CA); anti-myogenin (at 1:1000 dilution; Santa Cruz Biotechnology, Santa Cruz, CA); and polyclonal goat anti-human NCAM (at 1:400 dilution; Santa Cruz Biotechnology, Santa Cruz, CA) in 5% nonfat dry milk on TBST at 4 °C overnight. After washes with TBST, blots were incubated for 2 h with goat anti-rat peroxidase conjugated (Sigma, St Louis, MI) at 1:5000 dilution for nAChR $\alpha$ 7, avidin-peroxidase conjugated (BD-Pharmingen Biosciences, San Diego, CA) at 1:3000 dilution for TNF $\alpha$ , goat anti-rabbit peroxidase conjugated (Southern Biotechnology Associates Inc., Birmingham, AL) at 1:3000

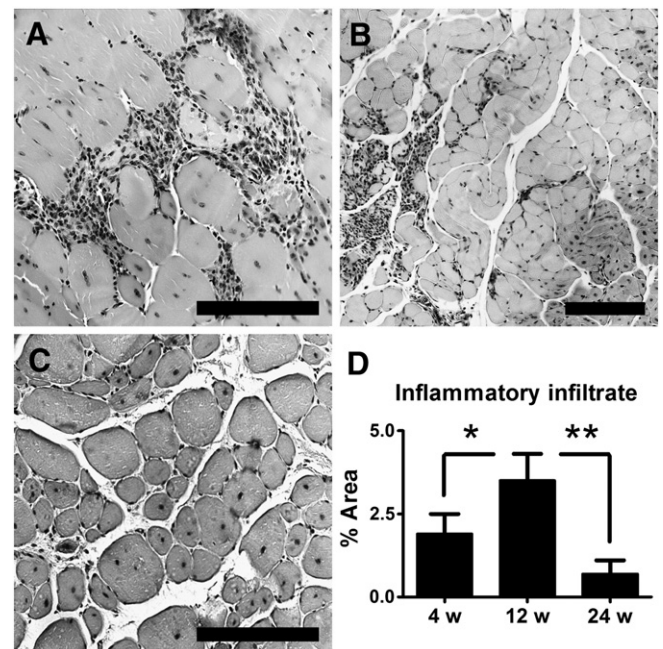


**Fig. 1.** Morphometric analysis of inflammatory infiltrates in *mdx* skeletal muscle. Histological analysis of *mdx* gastrocnemius muscles at (A) 4 weeks, (B) 12 weeks and (C) 24 weeks. Scale bar 100  $\mu$ m. (D) Percentage of inflammatory infiltrate area with statistical unpaired *t*-test analysis (\*  $p < 0.05$ ; \*\*  $p < 0.01$ ). Results from 5 animals per group are expressed as mean with standard deviation ( $\pm$ SD).

dilution for myogenin and rabbit anti-goat peroxidase conjugated (Sigma, St Louis, MI) at 1:5000 for NCAM.

Bands were identified with ECL Plus (Amersham Biosciences, Fairfield, CT) for chemiluminescent detection and subsequent film exposure for 5 min. Presence of proteins was verified by comparing protein bands to the Molecular Rainbow Weight Marker (Amersham Biosciences; Fairfield, CT). As negative controls, samples were incubated without primary antibodies. Equal loading of protein was assessed on stripped blots by immunodetection of  $\beta$ -actin using goat anti-human polyclonal peroxidase conjugated antibody diluted at 1:1000 (Santa Cruz Biotechnology, Santa Cruz, CA).

### 2.5. Reverse transcription-polymerase chain reaction (RT-PCR)

Total RNA from skeletal muscles was extracted using Trizol (Invitrogen, Carlsbad, CA) following the manufacturer's instruction.

Reverse transcription of 2  $\mu$ g RNA was performed using the pre-amplification system for first strand cDNA synthesis kit and SuperScript III RNase H-reverse transcriptase (Invitrogen, Carlsbad, CA). Mouse cDNA was amplified using recombinant Taq polymerase (Invitrogen, Brazil) and the primer sequences (Invitrogen, Carlsbad, CA) used to amplify mouse nAChR $\alpha$ 7, TNF $\alpha$  and  $\beta$ -Actin were the following: nAChR $\alpha$ 7, 5'-CGC TGG TTC CCT TTT GAT GTG-3' (forward) and 5'-ATG GTG CTG GCG AAG TAT TGT-3' (reverse); TNF $\alpha$ , 5'-GGC AGG TCT ACT TTG GAG TCA TTG C-3' (forward) and 5'-ACA TTC GAG GCT CCA GTG AAT TCG-3' (reverse); and  $\beta$ -Actin, 5'-AGC TGA GAG GGA AAT CGT GC-3' (forward) and 5'-GAT GGA GGG GCC GGA CTC AT-3' (reverse). A 3 min hot start at 94 °C was performed to denature the double strand cDNA. Amplification steps were the following: nAChR $\alpha$ 7 – 35 cycles (30 s at 94 °C, 60 s at 65 °C, and 60 s at 72 °C); TNF $\alpha$  – 30 cycles (45 s at 94 °C, 60 s at 62 °C, and 60 s at 72 °C); and  $\beta$ -Actin – 19 cycles (45 s at 94 °C, 45 s at 58 °C, and 60 s at 72 °C). All

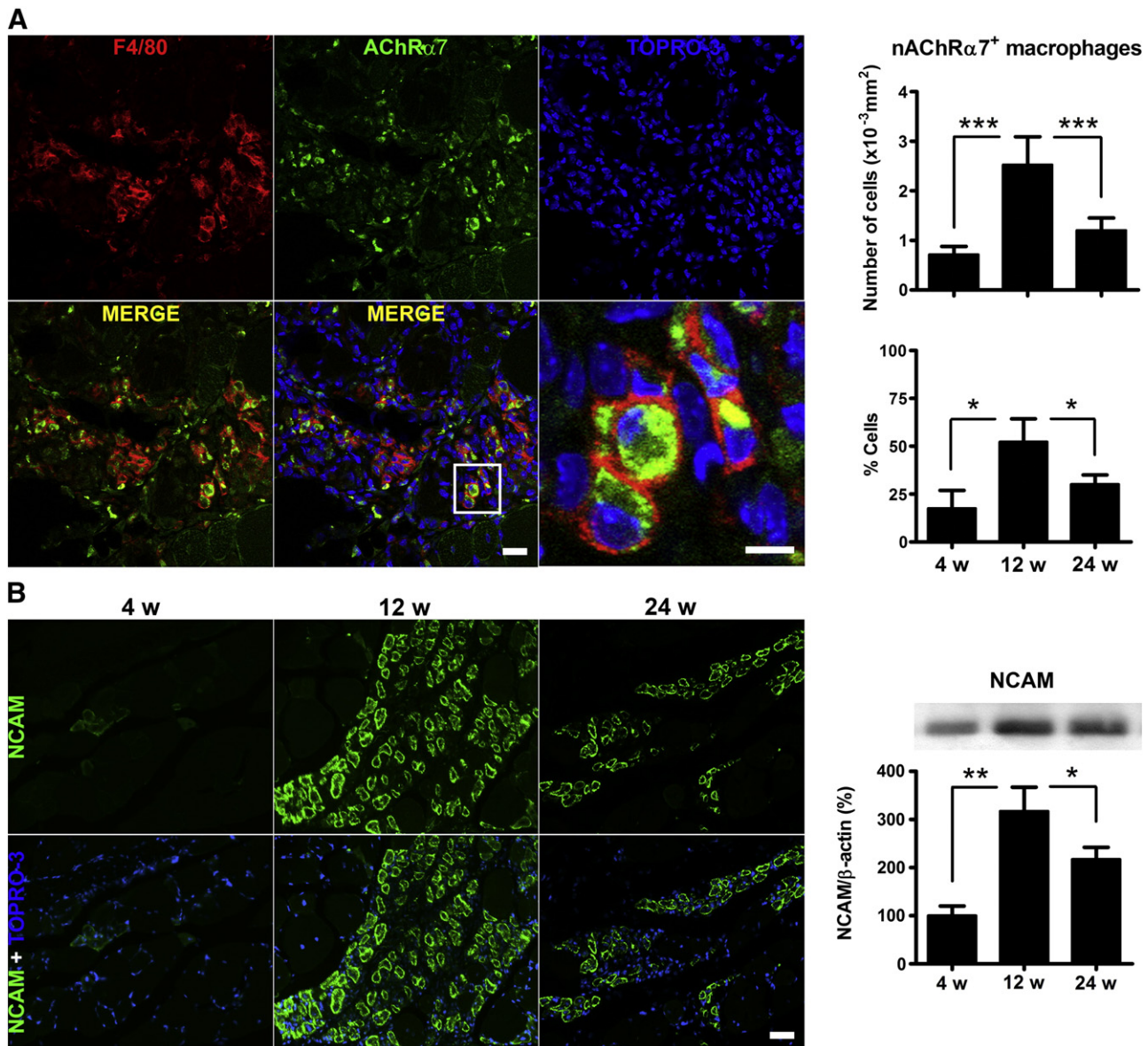


**Fig. 2.** Characterization of macrophages in *mdx* skeletal muscles. (A) Immunoreactivity of F4/80, nAChR $\alpha$ 7, TOPRO-3 nuclei counterstain and merged images without and with TOPRO-3 co-localization of nAChR $\alpha$ 7 and F4/80 of 12-week *mdx* skeletal muscles sections. High resolution merged images insert of indicated square in merged figure. Negative controls did not show immunoreactivity (images not shown). Scale bar 20  $\mu$ m, insert 6  $\mu$ m. On the right side,  $\times 10^{-3}$  cells per  $\mu\text{m}^2$  and percentage of the total F4/80 macrophages co-expressing nAChR $\alpha$ 7 in the inflammatory foci at different stages of the myopathy. One-way ANOVA test indicates  $p < 0.001$  and  $p < 0.05$ . (B) NCAM immunoreactivity of 4, 12 and 24 weeks and merged images with TOPRO-3 nuclei counterstain. Scale bar 20  $\mu$ m. The right side graphic depicts western blot analysis of NCAM expression. 43-kDa  $\beta$ -actin was used as loading control (image not shown). Statistical unpaired *t*-test analysis (\*  $p < 0.05$ ; \*\*  $p < 0.01$ ; \*\*\*  $p < 0.001$ ). It included 5 mice per group. Results are expressed as mean with standard deviation ( $\pm$ SD).

reactions were completed by a final amplification step at 72 °C for 5 min. The PCR products were resolved by electrophoresis on a 1.5% agarose gel with size standard  $\phi$ X174RF DNA Hae III Fragments (Invitrogen, Carlsbad, CA) at 130 V for 30 min and visualized by ethidium bromide staining.

## 2.6. Gelatin zymography

Gastrocnemius muscles from *mdx* and control mice were immediately frozen and preserved in liquid nitrogen. Muscles were homogenized (1/10 w/v) in Tris-buffered saline (TBS, 100 mM Tris-HCl, pH 7.6, 200 mM NaCl, 100 mM CaCl<sub>2</sub> and 1% Triton X-100). After centrifugation (12,000×g, 4 °C, 10 min), protein concentration in supernatant aliquots was determined by the Lowry method (Lowry et al., 1951), and equal amounts of total protein loaded for zymography (60 μg /lane). SDS-PAGE zymography was performed to determine gelatinase activity according to Heussen and Dowdle (Heussen and Dowdle, 1980). Briefly, zymogram gels consisted of 7.5% polyacrylamide-SDS impregnated with 2 mg/ml type A gelatin from porcine skin (Sigma, St. Louis, MI) and 4% polyacrylamide-SDS for stacking gels. Gels were further washed twice for 30 min in 2.5% Triton X-100 solution, then incubated at 37 °C for 24 h in substrate buffer (10 mM Tris-HCl buffer, pH 7.5 with CaCl<sub>2</sub> 5 mM, ZnCl<sub>2</sub> 1 μM). Thereafter gels were stained with 30% methanol/10% acetic acid containing 0.5% brilliant blue R-250 (Sigma, St Louis, MI). Gelatinase activity was visualized as unstained bands on a blue background, representing areas of proteolysis of the substrate protein.

Metalloproteases are secreted in a latent form and require cleavage of a NH<sub>2</sub> terminus peptide for activation. The exposure of proenzymes from tissue extracts to sodium dodecyl sulfate during gel separation leads to activation without proteolytic cleavage (Talhouk et al., 1992). Four bands can easily be seen corresponding to 100-kDa (MMP-9), 66-kDa (pre-pro-MMP-2), 60-kDa (pro-MMP-2) and 55-kDa (active-MMP-2) (Kherif et al., 1999).

## 2.7. In vivo treatment with nicotine

*Mdx* mice at 3 weeks (21 days postnatal, PN) received intraperitoneal injection of nicotine (400 μm/kg) or vehicle saline solution as previously described by van Maanen et al., 2009 (van Maanen et al., 2009) twice daily from day 21 PN until day 28 PN. At the end of treatment mice were sacrificed. At least 6 animals were included in each group.

## 2.8. Quantitative and statistical analysis

Quantitative analysis was performed using image-analysis software (Scion Image for Windows, Scion Corporation, National Institutes of Health; Bethesda, MD) for western blot, RT-PCR, zymography, morphometry and to quantify single and double-labeled macrophages per lesion area. GraphPad Prism 5 (GraphPad software Inc.) was used to calculate mean and standard deviations. One-way ANOVA and unpaired *t*-test was applied to obtain statistical significance of means. Differences were considered to be statistically significant at the 0.05 level of confidence.

## 3. Results

### 3.1. Analysis of the inflammatory infiltrate

Gastrocnemius muscles of *mdx* mice at 4 weeks showed few necrotic fibers and dense inflammatory infiltrates (Fig. 1A) which increased significantly at 12 weeks (84 ± 30%, *p* < 0.05) with areas containing regenerated myofibers, evidenced by central nucleation and basophilic cytoplasm (Fig. 1B). By 24 weeks, *mdx* muscles showed marked reduction of inflammatory infiltrates (80 ± 15%, *p* < 0.01) and extended areas with regenerated myofibers (Fig. 1C, D).

Presence of F4/80<sup>+</sup> nAChRα7<sup>+</sup> macrophages in the inflammatory foci was determined to establish a putative relation between nAChRα7 expression and inhibition of local inflammation. The inflammatory foci of *mdx* muscles at 12 weeks (Fig. 2A) presented 3.5-fold increase (52 ± 7%; *p* < 0.001) of F4/80<sup>+</sup> nAChRα7<sup>+</sup> macrophages per μm<sup>2</sup> in relation to *mdx* muscles at 4 weeks (18 ± 5%) and also 24 weeks (30 ± 3%). Muscular regeneration assessed by NCAM expression also correlated

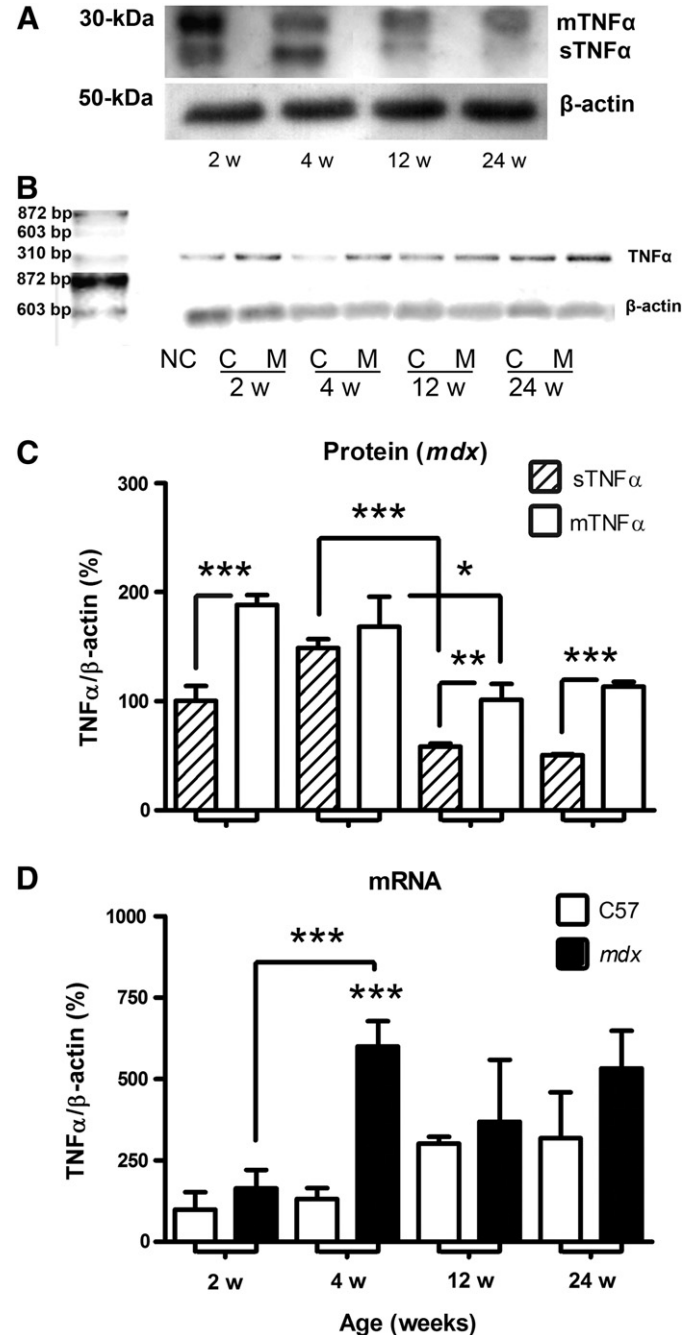


**Fig. 3.** TNFα protein and total mRNA expression in *mdx* skeletal muscles. (A) Western blot showing 27-kDa membrane TNFα and 17-kDa soluble TNFα forms in the gastrocnemius muscles of *mdx* mice, (B) Total RNA isolated from control C57, (C) and *mdx* (M) mice were reverse transcribed to cDNA by RT-PCR method, followed by PCR amplification of TNFα (see Material and Methods). Amplification efficiency was normalized to β-actin and PCR products were resolved by electrophoresis in 1.5% agarose gel. NC means Negative Control. (C) mTNFα and sTNFα protein levels in the gastrocnemius muscle of *mdx* mice. One-way ANOVA test for mTNFα and sTNFα forms (*p* < 0.001). (D) TNFα mRNA levels from C57 and *mdx*. One-way ANOVA test for TNFα mRNA of C57 (*p* < 0.05) and *mdx* (*p* < 0.001). Unpaired *t*-test analysis (\* *p* < 0.05; \*\* *p* < 0.01; \*\*\* *p* < 0.001). It included 5 mice per group. Results are expressed as mean with standard deviation (± SD).

with presence of nAChR $\alpha$ 7<sup>+</sup> F4/80 macrophages corresponding to a 3.2-fold increase ( $p < 0.005$ ) from 4 to 12 weeks and reduced levels at 24 weeks but still higher than 4 weeks (Fig. 2B).

### 3.2. Expression of mRNA and TNF $\alpha$ protein production in the skeletal muscle

Immunoblots showed two isoforms of TNF $\alpha$  (Fig. 3A), a non-cleaved 27-kDa form (mTNF $\alpha$ ) anchored to the cell membrane

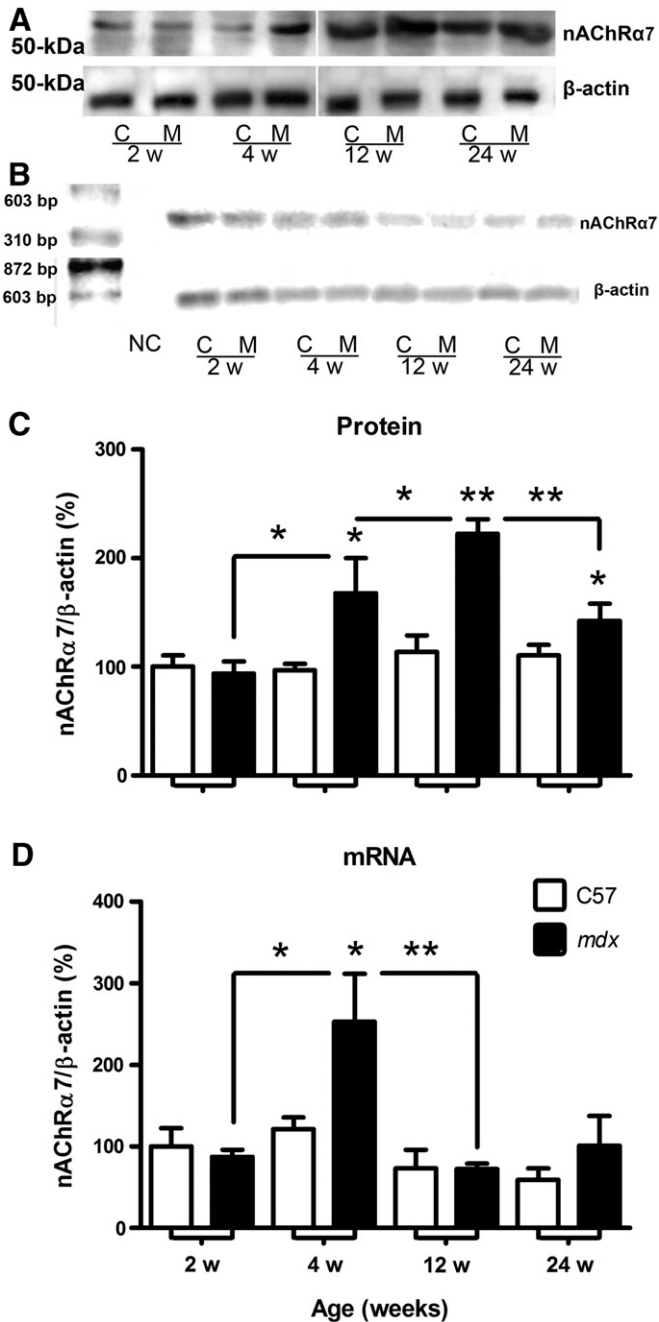


**Fig. 4.** nAChR $\alpha$ 7 protein and mRNA expression in *mdx* skeletal muscles. (A) Western blot showing nAChR $\alpha$ 7 protein and (B) nAChR $\alpha$ 7 mRNA expression in gastrocnemius muscles of both lineages. 43-kDa  $\beta$ -actin protein and mRNA were used as loading controls. C (C57), M (*mdx*) and NC (Negative Control). (C) Protein levels comparing nAChR $\alpha$ 7 content between C57 and *mdx* mice ( $n = 5$  mice per group) in the gastrocnemius muscles of *mdx* mice. One-way ANOVA test for nAChR $\alpha$ 7 protein indicates  $p < 0.05$  (C57) and  $p < 0.001$  (*mdx*). (D) nAChR $\alpha$ 7 mRNA levels from C57 and *mdx*. One-way ANOVA test for nAChR $\alpha$ 7 mRNA of C57 ( $p < 0.01$ ) and *mdx* ( $p < 0.001$ ). Unpaired *t*-test analysis (\*  $p < 0.05$ ; \*\*  $p < 0.01$ ). It included 5 mice per group. Results are expressed as mean with standard deviation ( $\pm$  SD).

involved in the induction of inflammation by cell-cell contact, acting as a receptor on TNF $\alpha$  producing cells through reverse or forward signaling (Domonkos et al., 2001; Xin et al., 2006) and 17-kDa form (sTNF $\alpha$ ), a product from protease cleavage and regarded as fine indicator of inflammation (Kherif et al., 1999). Confirming previous data, *mdx* mice at 2 and 4 weeks presented high expression of both isoforms with reduction from 12 weeks onwards (Bani et al., 2008), but the 17-kDa form was mainly observed during myonecrosis (Fig. 3C). These results indicate high proteolytic cleavage of 27-kDa membrane from 2 to 4 weeks ( $48 \pm 9\%$ ,  $p < 0.05$ ) followed by marked reduction at 12 weeks ( $61 \pm 3\%$ ,  $p < 0.001$ ) with levels remaining steady towards fibrosis (24 weeks). Despite presence of numerous macrophages at 12 weeks low TNF $\alpha$  production was observed. We further correlate mRNA expression with corresponding cytokine

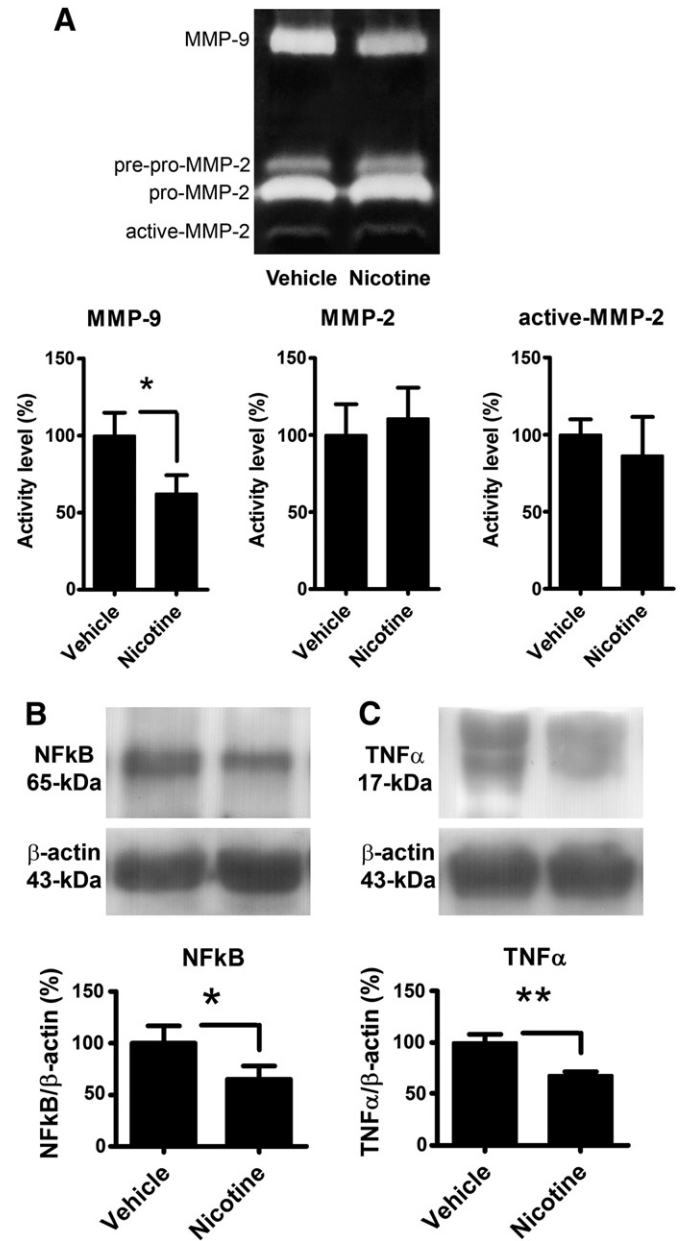


**Fig. 5.** Inhibition of inflammatory mediators by nicotine treatment. (A) Zymograms of metalloprotease activity from *mdx* muscles at 4 weeks. Graphs show the activity level of MMP-9, pro-MMP-2 and active-MMP-2 after intraperitoneal injection of nicotine. Western blot of (B) NF $\kappa$ B and (C) TNF $\alpha$  with respective graphs showing protein expression in the same tissue sample used for MMP analysis. 43-kDa  $\beta$ -actin protein was used as loading control. Unpaired *t*-test analysis (\*  $p < 0.05$ ; \*\*  $p < 0.01$ ). It included 6 mice per group. Results are expressed as mean with standard deviation ( $\pm$  SD).

production (Fig. 3B). C57 control mice at different ages consistently had low TNF $\alpha$  mRNA expression in gastrocnemius muscles. In contrast, *mdx* mice presented 3.7-fold increase from 2 to 4 weeks ( $p < 0.001$ ) corresponding to increased sTNF $\alpha$  production (Fig. 3D).

3.3. Expression of nAChR $\alpha$ 7 protein and mRNA in the skeletal muscle

Immunoblot analysis in gastrocnemius muscles homogenate revealed immunoreactive bands corresponding to nAChR $\alpha$ 7 (55-kDa) in both C57 and *mdx* gastrocnemius muscles (Fig. 4A). Control C57 non-dystrophic and *mdx* mice at 2 weeks showed similar nAChR $\alpha$ 7 protein content but *mdx* mice showed higher levels from 4 weeks ( $80 \pm 20\%$ ,  $p < 0.05$ ) until 12 weeks ( $138 \pm 11\%$ ,  $p < 0.001$ ) with a slight decline at 24 weeks ( $52 \pm 12\%$ ,  $p < 0.05$ ) (Fig. 4C). Expression of nAChR $\alpha$ 7 mRNA was relatively constant at selected ages of C57 gastrocnemius muscles (Fig. 4B) but *mdx* at 4 weeks showed high nAChR $\alpha$ 7 mRNA expression ( $190 \pm 21\%$ ,  $p < 0.01$ ) returning to previous levels at 12 weeks and 24 weeks (Fig. 4D).

3.4. Nicotine treatment downregulates pro-inflammatory mediators in *mdx* skeletal muscle

Gastrocnemius muscles of C57BL/10J control non-dystrophic mice had undetectable MMP-9 and active-MMP-2 activities but low levels (38%) of pro-MMP-2. In vivo treatment with 400  $\mu$ m/kg intraperitoneal

injection of nicotine reduced MMP-9 activity ( $38 \pm 11\%$ ;  $p < 0.05$ ) in relation to control sham *mdx* mice receiving vehicle. In vivo treatment of *mdx* mice with nicotine did not show any alteration regarding pro-MMP-2 and active-MMP-2 activities (Fig. 5A). Nicotine treatment further reduced NF $\kappa$ B ( $35 \pm 11\%$ ,  $p < 0.05$ , Fig. B) and TNF $\alpha$  ( $32 \pm 5\%$ ,  $p < 0.005$ , Fig. 5C) content in *mdx* muscles. Histological analysis confirmed that nicotine treatment reduced the inflammatory infiltrates ( $61 \pm 18\%$ ,  $p < 0.05$ , Fig. 6A) and increased myofiber regeneration assessed by area measurement of basophilic sarcoplasm and centrally located nuclei ( $28 \pm 9\%$ ,  $p < 0.05$ , Fig. 6B) without significant change in the pattern of myogenin expression (Fig. 6C) and collagen production (Fig. 6D).

4. Discussion

Excessive inflammation may lead to an increase in morbidity and mortality in several human diseases, although highly conserved endogenous mechanisms normally regulate the magnitude of innate immune responses. The nAChR $\alpha$ 7 subunit is considered a regulator of macrophage/monocyte activation for the release of molecules (TNF $\alpha$ , IL-1 $\beta$ , HMGB1) involved in inflammatory responses and apoptotic pathways (Pavlov and Tracey, 2005; Tracey, 2007; Ulloa, 2005; Wang et al., 2003; Yoshikawa et al., 2006). We present evidence that myofiber regeneration of *mdx* skeletal muscles is accompanied by increased numbers of F4/80 $^{+}$  macrophages, a sharp decrease of soluble TNF $\alpha$  and reduction of inflammatory infiltrates. Such results

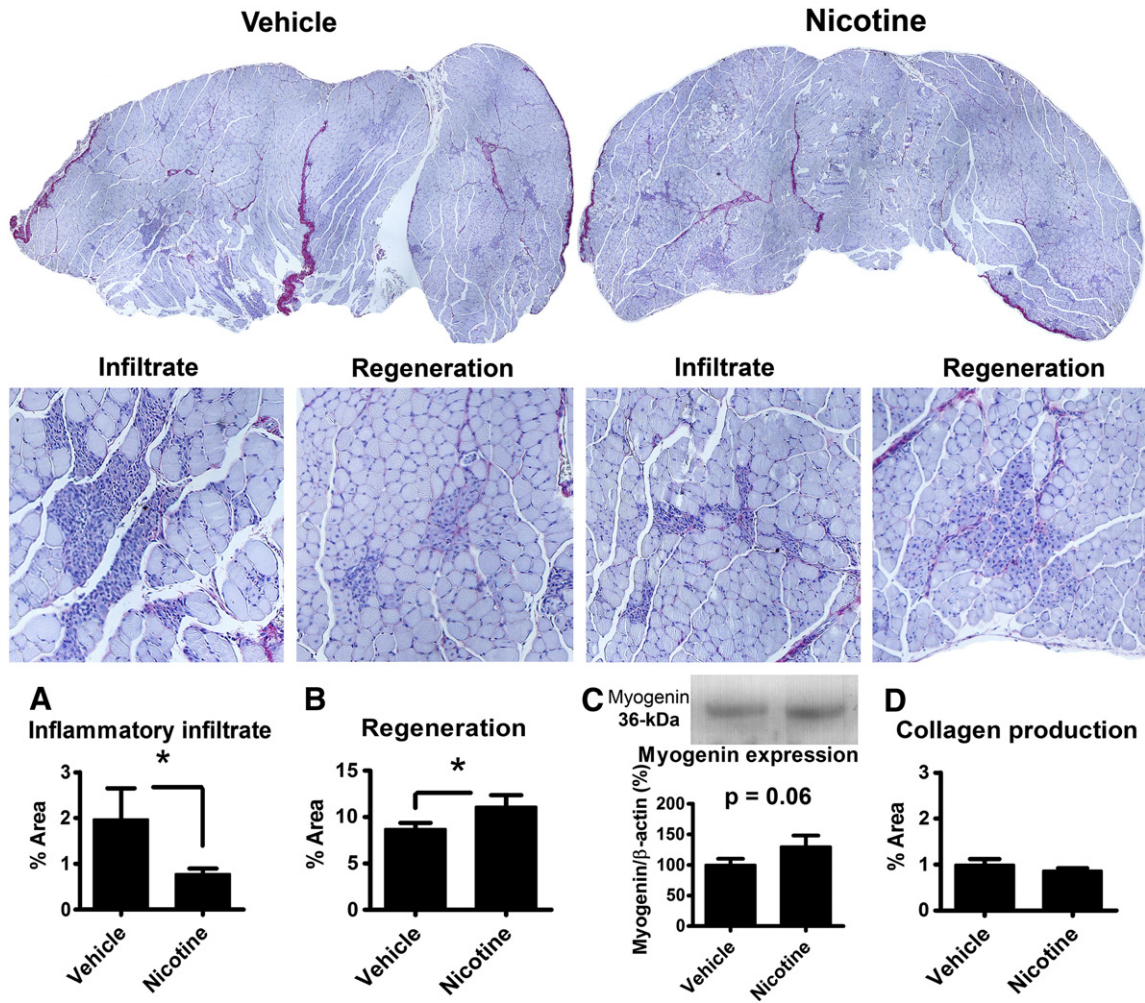


Fig. 6. Histological analysis of *mdx* skeletal muscles after nicotine treatment. On top, images from entire cross-section of vehicle and nicotine-treated *mdx* mice for 8 days. In the middle, high resolution images of the inflammatory infiltrate and regeneration area. Below, graphs showing quantification of areas with (A) inflammatory infiltrate, (B) regeneration, (C) myogenin expression and (D) collagen production. 43-kDa  $\beta$ -actin protein was used as loading control (image not shown). Unpaired *t*-test analysis (\*  $p < 0.05$ ). It included at least 5 mice in each experimental group. Results are expressed as mean with standard deviation ( $\pm$ SD).

suggest that similar function of the cholinergic anti-inflammatory pathway dependent upon acetylcholine secretion and nAChR $\alpha$ 7<sup>+</sup> macrophage activation described in other models (Bernik et al., 2002; Borovikova et al., 2000; Pavlov and Tracey, 2005; Pavlov and Tracey, 2006; Tracey, 2002; Tracey, 2007; Ulloa, 2005) is also attenuating inflammatory responses in *mdx* dystrophic muscles.

TNF $\alpha$  considered a major indicator of local inflammation is found either as a 27-kDa membrane-bound precursor or a 17-kDa mature soluble form produced by the protease action of TNF $\alpha$  converting enzyme (TACE) and MMP-9 (Kherif et al., 1999; Mullberg et al., 2000). Our results demonstrate that the 17-kDa TNF $\alpha$  form, which correlates with higher proteolytic cleavage, is increased during active myonecrosis of *mdx* gastrocnemius muscles, rather than at later stages of the disease.

TNF $\alpha$  synthesis, proteolytic processing and release of soluble cytokine are events strictly regulated at both transcriptional and translational levels. Indeed, results showing high TNF $\alpha$  mRNA and protein levels during the period of myonecrosis suggest a rapid translation. This is consistent with a putative dual role during inflammation leading either to muscle wasting by damaging existing muscle fibers (Rendon-Mitchell et al., 2003) and/or NF $\kappa$ B activation (Messina et al., 2006) which downregulates MyoD, a myogenic transcription factor essential for the formation of new muscle fibers (Guttridge et al., 2000). In this context efficient skeletal muscle repair in *mdx* dystrophic mice may greatly depend upon controlling local TNF $\alpha$  production. Indeed, pharmacological blockade of TNF $\alpha$  bioactivity greatly reduces the breakdown of dystrophic muscles (Grounds and Torrisi, 2004; Hodgetts et al., 2006). Interestingly low TNF $\alpha$  production despite the presence of numerous F4/80<sup>+</sup> nACh $\alpha$ 7<sup>+</sup> macrophages within the inflammatory foci was often associated with increased NCAM positive regenerating myofibers.

Similar to reports showing the anti-inflammatory effect of nAChR $\alpha$ 7 stimulation in mouse models of septic peritonitis and collagen-induced arthritis (van Maanen et al., 2009; van Westerloo et al., 2005), we also observed that nicotine treatment reduced *mdx* muscle inflammation (MMP-9, TNF $\alpha$ , NF $\kappa$ B), improved regeneration but did not increase collagen deposition or induce fibrosis. TNF $\alpha$  and IL1 $\beta$  cytokines secreted by activated macrophages up-regulate production of MMP-9 but not MMP-2, partly because NF $\kappa$ B and SP-1 binding sites are present in the promoter region of the MMP-9 gene but absent in the MMP-2 gene (Kherif et al., 1999). In addition metalloproteases play an important role in tissue remodelling by either promoting tissue destruction and leukocyte migration (e.g. MMP-9) (Li et al., 2009) or myofiber regeneration as described for MMP-2 (Kherif et al., 1999).

Besides neurons, acetylcholine may also be produced by immune cells, endothelial cells, amongst others (Rosas-Ballina et al., 2008). In this context, it is possible that acetylcholine derived from such sources or from the neuromuscular junction could be influencing the process of myonecrosis, muscular inflammation and myofiber regeneration in the *mdx* myopathy. Although skeletal muscles do not have parasympathetic innervations, our results indicate that F4/80<sup>+</sup> nAChR $\alpha$ 7<sup>+</sup> infiltrating macrophages have an important role in the control of *mdx* muscular lesion. Studies (Osborne-Herford et al., 2008) in a skin model of ultraviolet-induced lesion also showed that nAChR $\alpha$ 7 could modulate local pro-inflammatory response in the absence of parasympathetic innervations.

The present work shows that the anti-inflammatory effect of nAChR $\alpha$ 7 stimulation is partly related to the regulation of cytokine production by F4/80 macrophages and that in vivo nicotine treatment leads to muscular regeneration of *mdx* dystrophic mice. Future studies are necessary to evaluate the potential use of specific nAChR $\alpha$ 7 agonists, to determine their effects in mitigating myopathy and/or promoting activation of mechanisms related with efficient muscular regeneration.

## Acknowledgements

This study was supported by grants from CAPES (Coordenação de Aperfeiçoamento de Pessoal de Nível Superior), FOPESQ-UFF and

FAPERJ (Fundação de Amparo a Pesquisa do Rio de Janeiro). We thank Dr. Ricardo N. Isayama and Dr. Marcelo F. Santiago from the Institute of Biophysics Carlos Chagas Filho – UF RJ for generous help in tissue processing and confocal microscopy. We are grateful to Marcella d'Alincourt Salazar from the University of Toledo, Health Science Campus, Toledo, Ohio and Rosangela Lawrence from the Washtenaw Community College, Ann Arbor, Michigan, for the English revision.

## References

- Bani, C., Lagrota-Candido, J., Pinheiro, D.F., Leite, P.E., Salimena, M.C., Henriques-Pons, A., Quirico-Santos, T., 2008. Pattern of metalloprotease activity and myofiber regeneration in skeletal muscles of *mdx* mice. *Muscle Nerve* 37, 583–592.
- Bernik, T.R., Friedman, S.G., Ochani, M., DiRaimo, R., Ulloa, L., Yang, H., Sudan, S., Czura, C.J., Ivanova, S.M., Tracey, K.J., 2002. Pharmacological stimulation of the cholinergic antiinflammatory pathway. *J. Exp. Med.* 195, 781–788.
- Borovikova, L.V., Ivanova, S., Zhang, M., Yang, H., Botchkina, G.I., Watkins, L.R., Wang, H., Abumrad, N., Eaton, J.W., Tracey, K.J., 2000. Vagus nerve stimulation attenuates the systemic inflammatory response to endotoxin. *Nature* 405, 458–462.
- Carlson, C.G., 1998. The dystrophinopathies: an alternative to structural hypothesis. *Neurobiol. Dis.* 5, 3–15.
- Domonkos, A., Udvardy, A., Laszlo, L., Nagy, T., Duda, E., 2001. Receptor-like properties of the 26 kDa transmembrane form of TNF. *Eur. Cytokine Netw.* 12, 411–419.
- Evans, N.P., Misyak, S.A., Robertson, J.L., Bassaganya-Riera, J., Grange, R.W., 2009. Immune-mediated mechanisms potentially regulate the disease time-course of Duchenne muscular dystrophy and provide targets for therapeutic intervention. *PMR* 1, 755–768.
- Gotti, C., Clementi, F., 2004. Neuronal nicotinic receptors: from structure to pathology. *Prog. Neurobiol.* 74, 363–396.
- Grounds, M.D., Torrisi, J., 2004. Anti-TNF $\alpha$  (Remicade) therapy protects dystrophic skeletal muscle from necrosis. *FASEB J.* 18, 676–682.
- Guttridge, D.C., Mayo, M.W., Madrid, L.V., Wang, C.Y., Baldwin Jr., A.S., 2000. NF- $\kappa$ B-induced loss of MyoD messenger RNA: possible role in muscle decay and cachexia. *Science* 289, 2363–2366.
- Heussen, C., Dowdle, E.B., 1980. Electrophoretic analysis of plasminogen activators in polyacrylamide gels containing sodium dodecyl sulfate and copolymerized substrates. *Anal. Biochem.* 102, 196–202.
- Hodgetts, S., Radley, H., Davies, M., Grounds, M.D., 2006. Reduced necrosis of dystrophic muscle by depletion of host neutrophils, or blocking TNF $\alpha$  function with Etanercept in *mdx* mice. *Neuromuscul. Disord.* 16, 591–602.
- Kawashima, K., Fujii, T., 2003. The lymphocytic cholinergic system and its contribution to the regulation of immune activity. *Life Sci.* 74, 675–696.
- Khazen, W., M'Bika, J.P., Tomkiewicz, C., Benelli, C., Chany, C., Achour, A., Forest, C., 2005. Expression of macrophage-selective markers in human and rodent adipocytes. *FEBS Lett.* 579, 5631–5634.
- Kherif, S., Lafuma, C., Dehaupas, M., Lachkar, S., Fournier, J.G., Verdier-Sahuque, M., Fardeau, M., Alameddine, H.S., 1999. Expression of matrix metalloproteinases 2 and 9 in regenerating skeletal muscle: a study in experimentally injured and *mdx* muscles. *Dev. Biol.* 205, 158–170.
- Lagrota-Candido, J., Vasconcellos, R., Cavalcanti, M., Bozza, M., Savino, W.Q., Quirico-Santos, T., 2002. Resolution of skeletal muscle inflammation in *mdx* dystrophic mouse is accompanied by increased immunoglobulin and interferon- $\gamma$  production. *Intern. J. Exp. Pathol.* 83, 121–132.
- Lefaucier, J.P., Seville, A., 1996. Features of dystrophy in smooth and skeletal muscles of *mdx* mice. *Muscle Nerve* 19, 793–794.
- Li, H., Mittal, A., Makonchuk, D.Y., Bhatnagar, S., Kumar, A., 2009. Matrix metalloproteinase-9 inhibition ameliorates pathogenesis and improves skeletal muscle regeneration in muscular dystrophy. *Hum. Mol. Genet.* 18, 2584–2598.
- Lowry, O.H., Rosebrough, N.J., Farr, A.L., Randall, R.J., 1951. Protein measurement with the Folin phenol reagent. *J. Biol. Chem.* 193, 265–275.
- McGeachie, J.K., Grounds, M.D., 1999. The timing between skeletal muscle myoblast replication and fusion into myotubes, and the stability of regenerated dystrophic myofibers: an autoradiographic study in *mdx* mice. *J. Anat.* 194, 287–295.
- Messina, S., Bitto, A., Aguenouz, M., Minutoli, L., Monici, M.C., Altavilla, D., Squadrito, F., Vita, G., 2006. Nuclear factor kappa-B blockade reduces skeletal muscle degeneration and enhances muscle function in *mdx* mice. *Exp. Neurol.* 198, 234–241.
- Mullberg, J., Althoff, K., Jostock, T., Rose-John, S., 2000. The importance of shedding of membrane proteins for cytokine biology. *Eur. Cytokine Netw.* 11, 27–38.
- Nizri, E., Hamra-Amitay, Y., Sicsic, C., Lavon, I., Brenner, T., 2006. Anti-inflammatory properties of cholinergic up-regulation: a new role for acetylcholinesterase inhibitors. *Neuropharmacology* 50, 540–547.
- Osborne-Herford, A.V., Rogers, S.W., Gahring, L.C., 2008. Neuronal nicotinic alpha7 receptors modulate inflammatory cytokine production in the skin following ultraviolet radiation. *J. Neuroimmunol.* 193, 130–139.
- Pavlov, V.A., Tracey, K.J., 2005. The cholinergic anti-inflammatory pathway. *Brain Behav. Immun.* 19, 493–499.
- Pavlov, V.A., Tracey, K.J., 2006. Controlling inflammation: the cholinergic anti-inflammatory pathway. *Biochem. Soc. Trans.* 34, 1037–1040.
- Rendon-Mitchell, B., Ochani, M., Li, J., Han, J., Wang, H., Yang, H., Susarla, S., Czura, C., Mitchell, R.A., Chen, G., Sama, A.E., Tracey, K.J., 2003. IFN- $\gamma$  induces high mobility group box 1 protein release partly through a TNF-dependent mechanism. *J. Immunol.* 170, 3890–3897.
- Rosas-Ballina, M., Goldstein, R.S., Gallowitsch-Puerta, M., Yang, L., Valdes-Ferrer, S.I., Patel, N.B., Chavan, S., Al-Abed, Y., Yang, H., Tracey, K.J., 2009. The selective alpha7

- agonist GTS-21 attenuates cytokine production in human whole blood and human monocytes activated by ligands for TLR2, TLR3, TLR4, TLR9, and RAGE. *Mol. Med.* 15, 195–202.
- Rosas-Ballina, M., Ochani, M., Parrish, W.R., Ochani, K., Harris, Y.T., Huston, J.M., Chavan, S., Tracey, K.J., 2008. Splenic nerve is required for cholinergic antiinflammatory pathway control of TNF in endotoxemia. *Proc. Nat. Acad. Sci. U.S.A.* 105, 11008–11013.
- Saeed, R.W., Varma, S., Peng-Nemeroff, T., Sherry, B., Balakhaneh, D., Huston, J., Tracey, K.J., Al-Abed, Y., Metz, C.N., 2005. Cholinergic stimulation blocks endothelial cell activation and leukocyte recruitment during inflammation. *J. Exp. Med.* 201, 1113–1123.
- Shytle, R.D., Mori, T., Townsend, K., Vendrame, M., Sun, N., Zeng, J., Ehrhart, J., Silver, A.A., Sanberg, P.R., Tan, J., 2004. Cholinergic modulation of microglial activation by alpha 7 nicotinic receptors. *J. Neurochem.* 89, 337–343.
- Talhok, R.S., Bissell, M.J., Werb, Z., 1992. Coordinated expression of extracellular matrix-degrading proteinases and their inhibitors regulates mammary epithelial function during involution. *J. Cell Biol.* 118, 1271–1282.
- Tayebati, S.K., Amenta, F., El-Assouad, D., Zaccheo, D., 2002. Muscarinic cholinergic receptor subtypes in the hippocampus of aged rats. *Mech. Ageing Dev.* 123, 521–528.
- Torres, L.F., Duchon, L.W., 1987. The mutant *mdx*: inherited myopathy in the mouse. Morphological studies of nerves, muscles and end-plates. *Brain* 110 (Pt 2), 269–299.
- Tracey, K.J., 2002. The inflammatory reflex. *Nature* 420, 853–859.
- Tracey, K.J., 2007. Physiology and immunology of the cholinergic antiinflammatory pathway. *J. Clin. Invest.* 117, 289–296.
- Ulloa, L., 2005. The vagus nerve and the nicotinic anti-inflammatory pathway. *Nat. Rev. Drug Discov.* 4, 673–684.
- van Maanen, M.A., Lebre, M.C., van der Poll, T., LaRosa, G.J., Elbaum, D., Vervoordeldonk, M.J., Tak, P.P., 2009. Stimulation of nicotinic acetylcholine receptors attenuates collagen-induced arthritis in mice. *Arthritis Rheum.* 60, 114–122.
- van Westerloo, D.J., Giebelen, I.A., Florquin, S., Daalhuisen, J., Bruno, M.J., de Vos, A.F., Tracey, K.J., van der Poll, T., 2005. The cholinergic anti-inflammatory pathway regulates the host response during septic peritonitis. *J. Infect. Dis.* 191, 2138–2148.
- Voisin, V., de la Porte, S., 2004. Therapeutic strategies for Duchenne and Becker dystrophies. *Int. Rev. Cytol.* 240, 1–30.
- Wang, H., Yu, M., Ochani, M., Amella, C.A., Tanovic, M., Susarla, S., Li, J.H., Yang, H., Ulloa, L., Al-Abed, Y., Czura, C.J., Tracey, K.J., 2003. Nicotinic acetylcholine receptor alpha7 subunit is an essential regulator of inflammation. *Nature* 421, 384–388.
- Williams, S., Jacobson, C., 2010. Alpha-dystroglycan is essential for the induction of Egr3, a transcription factor important in muscle spindle formation. *Dev. Neurobiol.* 70 (7), 498–507.
- Xin, L., Wang, J., Zhang, H., Shi, W., Yu, M., Li, Q., Jiang, X., Gong, F., Gardner, K., Li, Q.Q., Li, Z., 2006. Dual regulation of soluble tumor necrosis factor-alpha induced activation of human monocytic cells via modulating transmembrane TNF-alpha-mediated 'reverse signaling'. *Int. J. Mol. Med.* 18, 885–892.
- Yoshikawa, H., Kurokawa, M., Ozaki, N., Nara, K., Atou, K., Takada, E., Kamochi, H., Suzuki, N., 2006. Nicotine inhibits the production of proinflammatory mediators in human monocytes by suppression of I-kappaB phosphorylation and nuclear factor-kappaB transcriptional activity through nicotinic acetylcholine receptor alpha7. *Clin. Exp. Immunol.* 146, 116–123.